

# Meteoric CaO and carbon smoke particles collected in the upper stratosphere from an unanticipated source

By VINCENZO DELLA CORTE<sup>1\*</sup>, FRANCISCUS J. M. RIETMEIJER<sup>2</sup>,  
ALESSANDRA ROTUNDI<sup>1</sup>, MARCO FERRARI<sup>1</sup> and  
PASQUALE PALUMBO<sup>1</sup>, <sup>1</sup>*Dipartimento di Scienze Applicate, Università degli Studi di Napoli  
"Parthenope", Centro Direzionale, I C4, Napoli 80143, Italy;* <sup>2</sup>*Department of Earth and Planetary Sciences,  
MSC03 2040, I-University of New Mexico, Albuquerque, NM 87131, USA*

(Manuscript received 27 November 2012; in final form 2 June 2013)

## ABSTRACT

Nanometre CaO and pure carbon smoke particles were collected at 38-km altitude in the upper stratosphere in the Arctic during June 2008 using DUSTER (Dust in the Upper Stratosphere Tracking Experiment and Retrieval). This balloon-borne instrument was designed for non-destructive collection of solid particles between 200 nm to 40  $\mu\text{m}$ . We report here on micrometre CaCO<sub>3</sub> (calcite) grains with evidence of thermal erosion and smoke particles that formed after melting and vaporisation and complete dissociation of some of the CaCO<sub>3</sub> grains at temperatures of approximately 3500 K. These conditions and processes suggest that the environment of this dust was a dense dust cloud that had formed after disintegration of a carbonaceous meteoroid during deceleration in the atmosphere. The balloon-borne collector must have coincidentally travelled through the dust cloud of a recent bolide event that had penetrated between 38.5 and 37 km altitude. This work identified a previously unknown meteoric smoke forming process in addition to meteoric smoke particles due to photolysis-driven oxidation of mesospheric metals from meteor ablation that had settled into the upper stratosphere.

*Keywords: meteoric smoke, carbonaceous meteorites, stratospheric dust, laboratory analyses, chemical composition*

## 1. Introduction

Solid and condensed nanometre- to micrometre-size particles in the upper stratosphere originate from both terrestrial and extra-terrestrial sources. It is generally thought that this region of the stratosphere is dominated by extra-terrestrial particles and that terrestrial debris, mostly volcanic ash ejecta, is more prevalent in the lower stratosphere. However, an injection of nano and micrometre volcanic ash particles due to the 1982 El Chichón volcanic eruption was collected in the upper stratosphere between 34 and 36 km altitudes during May 1985 (Testa et al., 1990; Rietmeijer, 1993). Volcanic ash particles tend to be mostly irregular mineral fragments and mineral clusters often with condensed nanoparticles such as NaCl and KCl salts and

sulfuric acid at their surface. With a tremendous literature database that is available on the morphology, mineralogy and chemistry of explosive volcanic ash ejecta (among many others, Rose et al., 1980, 1982; Farlow et al., 1981; Pueschel et al., 1994), the identification of volcanic dust collected in the stratosphere is not a problem.

Condensed particles can also be the result of meteor ablation. Meteoric dust in bolides is occasionally deposited into the lower stratosphere around 20-km altitude (Jenniskens, 2006). Meteoric smoke particles with predicted radii ranging from 0.2 to 10 nm (Hunten et al., 1980) form a haze layer in the mesosphere and stratosphere from  $\sim$ 85 km to about 35 km altitudes (Hervig et al., 2009). Meteors are common daily events but only a fraction of this incoming extra-terrestrial mass is recovered at the Earth's surface because meteoroids decelerating in the atmosphere will typically lose about 85% of their mass but they are not completely vaporised ('shooting stars') (Rietmeijer, 2000). In fact, the annual  $(40 \pm 20) \times 10^6$  kg terrestrial mass

\*Corresponding author.  
email: vincenzo.dellacorte@uniparthenope.it

accretion rate is due to micrometeorites ranging from 10 to 500  $\mu\text{m}$  in diameter (Love and Brownlee, 1993). When the temperatures are high enough, surface ablation of a decelerating meteoroid produces fragments, liquid droplets and vapours that are deposited in the atmosphere (Murad and Williams, 2002; Hawkes et al., 2005; Klekociuk et al., 2005; Borovička and Charvát, 2009). Meteorites and micrometeorites are collected at the Earth's surface (Murad and Williams, 2002), but so far condensed meteoric smoke particles have escaped in situ collection in the upper stratosphere and laboratory identification albeit not for a lack of trying.

During the 1950s and 1960s, balloons and high-flying aircraft carried dust collectors into the stratosphere (Bigg et al., 1970, 1971; Bigg, 2012) and the lower thermosphere (Hemenway and Soberman, 1962) for the purpose of collecting noctilucent cloud particles and meteoric dust (Hemenway et al., 1964). These collection efforts recovered solid spheres, fragments and smoke particles, typically between  $\sim 200$  nm and  $\sim 5$   $\mu\text{m}$ ; some of the material was crystalline (Hemenway and Soberman, 1962; Hemenway et al., 1964; Witt et al., 1964; Bigg et al., 1970, 1971). The dust compositions included (1) Al, Si, (2) Fe, Ti, Mg, Ca, (3) Al, Si, Fe, (4) Ti, Ca with minor Mg, Fe, Si, as well as organic particles (Bigg, 2012), but these element combinations cannot be used to constrain particle origins, for example volcanic dust, meteoric debris or anthropogenic dust. A meteoric origin for these particles rather than a terrestrial origin was usually inferred from the very high collection altitudes, reasoning that terrestrial air-borne dust would not reach the upper stratosphere. An extra-terrestrial origin of this early collected stratospheric dust was tenuous albeit not necessarily incorrect. The lack of success of these early attempts was compromised by the absence of suitable analytical techniques to characterise individual nano- and micrometre-scale particles that made it virtually impossible to recognise such small anthropogenic and natural terrestrial dust particles (Bigg, 2012). Where then are the hypothesised metal-oxide meteoric smoke particles and what are their mineralogical and chemical properties?

Only routine dust collection campaigns will confirm the existence of this putative terrestrial and extra-terrestrial stratospheric dust stratification, but more importantly they will contribute to a solid database of the natures of the transient and semi-permanent stratospheric nanometre and micron-sized dust species. To this purpose DUSTER (Dust in the Upper Stratosphere Tracking Experiment and Retrieval) was developed for the non-destructive and uncontaminated collection of micron size and smaller particles in situ in the upper stratosphere for laboratory analyses using state-of-the-art techniques (Della Corte et al., 2011, 2012). We report the first collection of meteoric CaO and pure carbon particles in the upper stratosphere.

## 2. Dust collector and analyses

Contamination is the bane of all small particle collections in Earth's upper stratosphere, which is still very much *terra incognita* with respect to the nature of its dust loading. DUSTER is a balloon-borne instrument for the non-destructive collection of particles between 200 nm to 40  $\mu\text{m}$  in the upper stratosphere between 30 and 40 km altitude ( $\sim 12$ – $3$  mbar). It is an active sampling system that was specifically developed to minimise and to control contamination during autonomous flight performance. The assembled instrument itself consists of: (1) an inlet tube, (2) a collecting chamber (3), an actual collector (4) the operational blank collector, and (5) a pumping system (Della Corte et al., 2012). The operational blank collector is mounted in a smaller chamber but in communication with the collection chamber. The air flux with entrained particles does not impinge on the blank; no stratospheric particles can be deposited on the blank. The blank collector serves two different purposes, *viz.* (1) a monitoring surface to identify particles that are deposited on the collectors during assembling and disassembling of DUSTER and when placing the collectors in or removing from the sample chamber of the Field Emission Scanning Electron Microscope (FESEM) that is not installed in a clean room, and (2) detection of accidental contamination events when the collection chamber is in the sealed configuration [e.g. air inlets due to leakage of ultra-high-vacuum (UHV) valves].

All mechanical parts of the collecting chamber including the actual and the blank collectors were cleaned and assembled in a Class 100 clean room. Two UHV valves isolate the collecting chamber from the ambient environment throughout the assembling phase, the balloon launch, during the flight when the DUSTER is inactive and the disassembling phase performed inside the clean room. The instrument inlet pipe was cleaned and integrated in the clean room, and connected on one side to the valve sealing the collecting chamber and on the other side sealed by a ConFlat 40 flange. This flange stayed fixed to the inlet during all pre-flight operations in the laboratory, during transportation and at the balloon launch site. It is released by a one-shot mechanism when the balloon reaches about 20-km altitude when DUSTER is above the tropopause and most of the terrestrial air-borne dust, and above the altitudes of the NASA Cosmic Dust Program (Zolensky et al., 1994). During ascent the balloon expands and goes through quite large temperature changes when crossing the tropopause. In the older balloon-borne campaigns that sampled stratospheric dust, this potential source of 'self-contamination' due to the release of surface and tropospheric dust adhered to the balloon surface was considered a serious uncontrollable source of contamination. This flange isolates the inlet tube from the ambient environment

during its initial ascent to 20-km altitude thus shielding the entire DUSTER system from contamination with tropospheric and lower stratospheric dust and dust that might have detached from the balloon skin. After the release of this flange, the UHV valve of the collecting chamber is still closed and DUSTER is not yet actively sampling the stratosphere. Pressure sensors control the active sampling period by opening and closing the UHV valves that are pre-set for the desired collection altitudes. Stratospheric dust is sampled actively at a low speed for inertial separation that decouples the dust flux from the atmospheric gas at altitude. Particles entering the inlet tube are deposited directly onto holey carbon thin-film substrates supported by Au mesh grids located on the actual collector that is positioned perpendicular to the airflow. The actual and blank collectors each contain 14 numbered grids held in place by a gold-coated mask (Della Corte et al., 2011, 2012).

During the pre-flight preparations before mounting the actual and blank collectors inside the collecting chamber, both collectors were completely scanned for the presence of any particles using an automated procedure to obtain high-resolution images with a FESEM. The complete scans of the actual and blank substrates produced about 150,000 images; the images are stitched together to create a mosaic image of each grid. This high-resolution imaging procedure provided a complete characterisation and record of any pre-existing particles with a diameter  $>100$  nm present prior to stratospheric sampling. The ZEISS Supra FESEM operated at accelerating voltages from 2 to 4 kV to optimise image resolution with respect to charging of the uncoated particles. The FESEM is equipped with an Oxford INCA Energy 350 system with a Si(Li) INCA X-sight PREMIUM EDX (energy-dispersive X-ray) detector operating at an accelerating voltage of 10 keV for chemical analyses of the particles. At these conditions, this instrument allows the detection of  $K_{\alpha}$  peaks of elements with atomic number 6 (C) to 22 (Ti) and of L and M peaks of elements with atomic number  $>22$ .

After completion of the collection flight, both the flight operational blank and the actual collectors were re-analysed following the same FESEM procedures. When the blank's integrity was compromised during the actual period of stratospheric collection, or at any time after closing the actual collector during descent, recovery or transportation to the laboratory in Naples, these added particles (relative to the pre-flight analyses) are proof of contamination. When the blank's integrity was preserved, the difference between pre- and post-flight dust loadings on the actual collector are particles that were collected in the upper stratosphere. The actual collector then becomes the permanent sample holder for subsequent analyses of the collected particles, which avoids particle manipulation

and post-collection contamination. The post-flight FESEM procedure found only two particles on the blank collector. Both particles show morphologies and compositions that are completely different from those found on the actual collector. They resemble particles used in other aerosol experiments conducted in the laboratory and were probably deposited on the blank collector in the FESEM room.

### 3. Results

DUSTER was launched from Svalbard (Norway;  $\sim 78^{\circ}\text{N}$ ) at 4 am on 21 June 2008, and sampling started about 2 hours later. After 55 hours of continuous sampling, the stratosphere between 37 and 38.5 km altitude DUSTER was switched off at 7:30 pm on 24 June 2008, and the collecting chamber was sealed prior to descent and recovery of DUSTER in Thule (Greenland;  $\sim 72^{\circ}\text{N}$ ). The instrument sampled  $6.6\text{ m}^3$  of ambient atmosphere at a  $0.12\text{ m}^3/\text{h}$  effective flow rate.

DUSTER collected 25 particles that range from 0.4 to  $\sim 9\text{ }\mu\text{m}$  with a single large outlier, an aggregate of  $\sim 25\text{ }\mu\text{m}$  in size (Fig. 1). During FESEM analysis, this large aggregate (D08\_003; Ciucci, 2011; Ciucci et al., 2011) fragmented into numerous tiny fragments some of which are still visible underneath the holey carbon film where they are inaccessible to further FESEM analyses except for two micrometre Ca–C–F particles. Two large particles of the main group of sub-equant and platy grains (Fig. 1) are calcite and/or aragonite (De Angelis et al., 2011). Although they appear to be massive they show the rotten and texturally laminated (i.e. layered) appearance due to thermal erosion (Rietmeijer et al., 2003b). The grain surfaces can be smooth due to a thin surface melt layer or be covered by numerous nanospheres.

The smallest particles ( $<2\text{ }\mu\text{m}$ ) are mostly platy grains, an aggregate of pure carbon nanograins (Fig. 2) and a porous aggregate of Ca[O] nanograins (Fig. 3). The carbon aggregate consists of individual grains ranging from 10 to 70 nm. It is surrounded by what appears to be a spray zone of carbon nanograins ranging from 10 to 50 nm in size on the holey carbon film surrounding the main aggregate. Some of the grains in the spray zone had fused into tiny clusters, which could account for the largest of these nanograins and possibly also for some of the smallest grains in the main aggregate. The EDX data show that this aggregate contains only carbon. We note that the ultrathin support film does not contribute to the detected carbon signature of this aggregate particle but it does contribute approximately 5 at % oxygen. The post-flight support film shows a very low but persistent oxygen background for which the particle spectra were corrected. The origin of this O-background is unknown but it was acquired during stratospheric sampling.

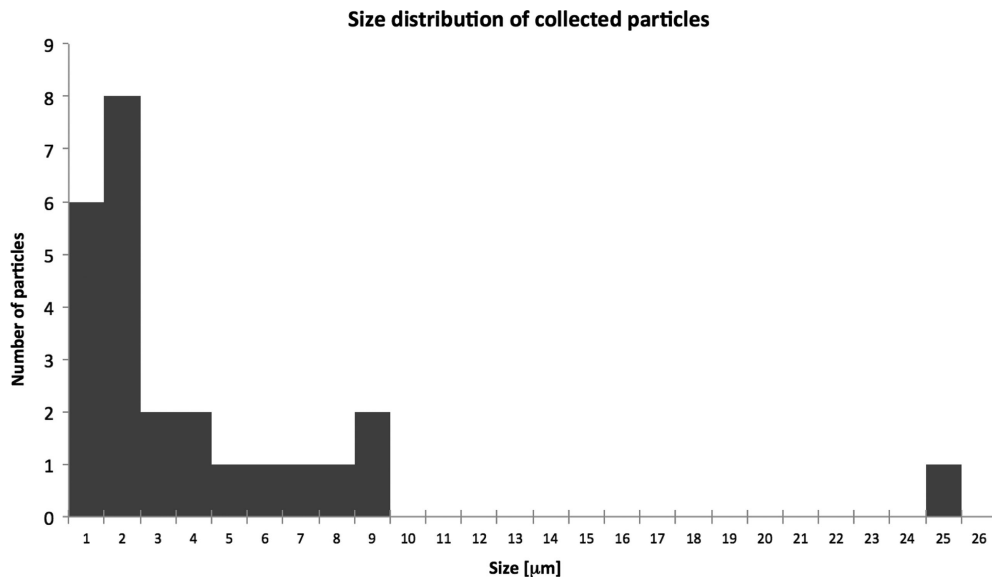


*Fig. 1.* Size distribution (microns) of the particles collected between 37 and 38.5 km during June 21–24, 2008 between  $\sim 72^\circ\text{N}$  and  $\sim 78^\circ\text{N}$  (modified after Della Corte et al., 2012).

The individual spherical nanograins in this porous aggregate particle range from  $\sim 10$  to  $\sim 120$  nm, that appear to have accreted onto a larger grain of 250 nm in diameter (Fig. 3). The largest sphere is probably a melted carbonate grain that developed small pores when  $\text{CO}_2$  escaped during calcite decomposition, *viz.*  $\text{CaCO}_3 \rightarrow \text{CaO} + \text{CO}_2$ . Most likely the gas-phase reactions also included  $\text{CO}_2 = \text{C}_{\text{gas}} + \text{O}_2$  and  $\text{C}_{\text{gas}} = \text{C}_{\text{solid}}$  at temperatures that exceeded the decomposition temperature (Sugita and Schultz, 1999).

The smallest grains are approximately 10 nm in diameter which is similar to the largest size of meteoric smoke particles (Hunten et al., 1980). The only available grain size data for context the grain size distributions of the pure carbon and Ca[O] nanoparticles are the grains sizes of Fe(Ni) nanometeorites (Hemenway et al., 1961) (Fig. 4). There is considerable overlap of the largest Fe(Ni) nanometeorites and the smallest pure carbon and Ca[O] nanograins. The grain size distributions for these nanoparticles indicate that grain growth occurred by simple surface free-energy-driven Ostwald ripening (Baronnet, 1984).

The Ca[O] notation signifies that these nanograin compositions were not measurable directly because: (1) their very small mass prohibited the acquisition of a statistically significant EDX signal, and (2) the signal was washed out by an omnipresent iron source. This source was a steel pin that had been placed inadvertently too close to the collection surfaces (Ciucci et al., 2011). This Fe-source is used as a reference to constrain the porous smoke aggregate D08\_031 compositions and their measured

compositions are shown along with the collector background composition (Fig. 5). The ‘in-hole’ analyses were obtained by placing the analytical FESEM probe over holes in the supporting thin film. They represent the post-collection DUSTER background. These data define a linear trend that would intersect the Fe–O join (Fig. 5) at about 50%. As the porous smoke aggregate (D08\_031) data are also on this mixing line, they show that the aggregate particles contain very little if not zero carbon, but they do contain oxygen.

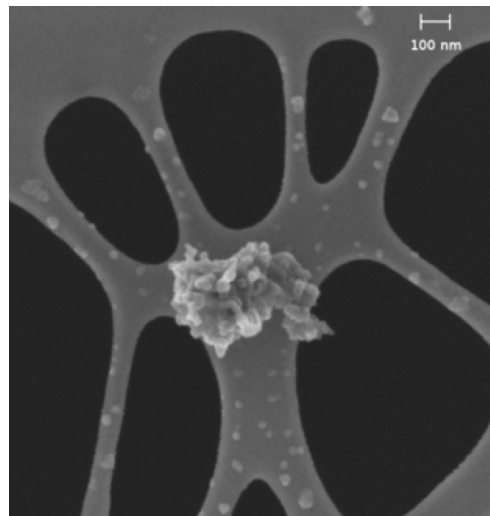


*Fig. 2.* A FESEM image of pure carbon aggregate of numerous nanograins (D08\_033) supported on the holey carbon film used for dust collection. The aggregate is about 300 nm in size. It is surrounded by a spray zone of smaller carbon nanograins.

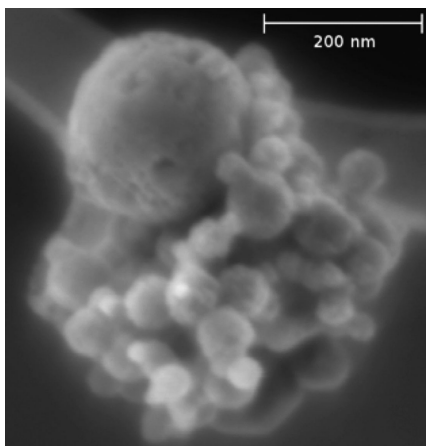


Fig. 3. A FESEM image showing porous aggregate (D08\_031) consisting of condensed Ca[O] nanograins that are accreted onto a larger melted aggregate of tiny carbonate grains. Small pores are visible in the largest sphere. The entire cluster is about 425 nm in size. The background is the holey carbon thin-film collection substrate.

To constrain the cation, we relied on the commonality of Ca–C–O compositions of the collected particles and the presence of the 5–7  $\mu\text{m}$   $\text{CaCO}_3$  carbonate grains. The Ca[O] nanospheres resemble those produced in a low-angle impact experiment that caused the thermal decomposition of dolomite,  $\text{CaMg}(\text{CO}_3)_2$  (Sugita and Schultz, 1999) and the formation of MgO and CaO nanospheres most often with a pure carbon rim. An analytical transmission electron microscope study showed that they are mostly  $< 50$  nm in diameter but with a range from 4 to  $\sim 200$  nm. When not

coated with a carbon rim, the nanospheres formed globular clusters up to  $\sim 500$  nm in diameter (Rietmeijer et al., 2003b). We reanalysed some of these nanospheres using the same FESEM conditions that were used to characterise particles D08\_031 and D08-033. Using the same experimental conditions, the instrument detected a weak CaO signal in a nanosphere from this hypervelocity impact experiment (Fig. 6). It did not detect either MgO or CaO in a smaller 270-nm sphere from the same impact experiment.

This difference using FESEM could be due to a shielding effect of a carbon rim, or because the core was too small (very low mass). It was found that the FESEM conditions used to analyse the collected aggregate means that Ca and Mg can only be analysed quantitatively in spheres  $\geq 1$   $\mu\text{m}$  in diameter. The size of aggregate particle D08\_31 (Fig. 3) is within the range wherein a FESEM signal is too weak to be detectable. Within the compositional constraints of the collected particles, we submit that the nanograins in this aggregate are CaO, possibly covered by a thin carbon layer.

#### 4. Discussion

We report the first collection of meteoric particles in the upper stratosphere during June 2008, which is an unfavourable time of the year to collect meteoric smoke particles in the Arctic and the reason why so few particles were collected. All DUSTER procedures were designed to eliminate collected particle contamination and in this regard the experiment was highly successful during operation between 37 and 38.5 km altitude. Still, it does not automatically guarantee an extra-terrestrial origin, or that

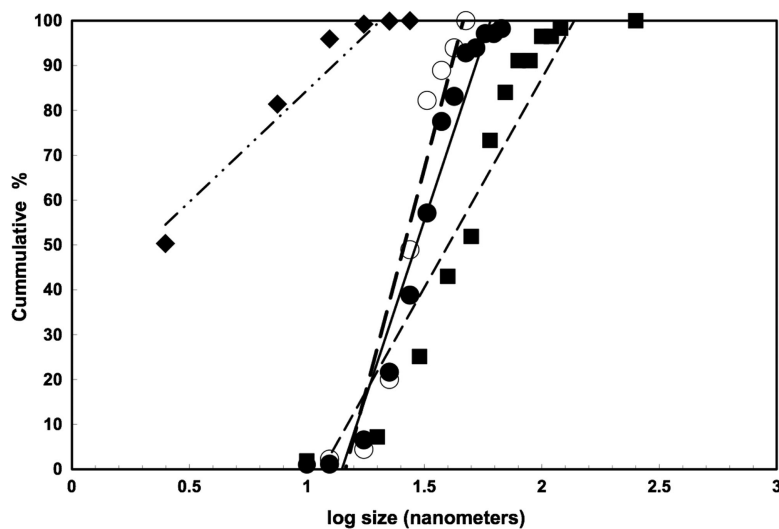
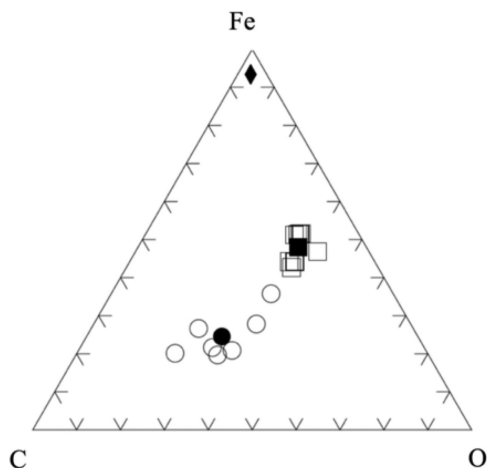


Fig. 4. Lognormal size distributions for the condensed Ca[O] nanograins in aggregate particle D08\_031 (Fig. 3) (solid squares) and the pure carbon nanograins in the aggregate smoke particle D08\_033 (dots) and deposited on the support film (open circles) (Fig. 2) compared to the size distribution of Fe(Ni) nanometeorites collected in the lower stratosphere (diamonds) (Hemenway et al., 1961). All linear correlation coefficients ( $r^2$ ) are  $\geq 0.9$ .



*Fig. 5.* The Fe–C–O (at %) ternary diagram showing the composition of the porous smoke aggregate particle D08\_031 (squares) and ‘in-hole’ analyses (circles) when the electron beam was placed across a hole in the holey carbon support film of the collector. These analyses represent a collector background composition. Iron in this diagram (diamond) results from a steel pin that is located directly below the actual collector (Ciucci, 2011; Ciucci et al., 2011). The open symbols are individual analyses; solid symbols are average compositions.

the collected particles can be linked to meteor ablation processes. A key diagnostic to derive an origin is that all of the collected particles have a Ca–C–O composition (Ciucci, 2011). Other possible origins include anthropogenic sources, such as aircraft and space-related activities. In this regard, the NASA Johnson Space Center Cosmic Dust Catalogs are a valuable resource as they categorise dust particles collected at 17–19 km altitude as either extra-terrestrial, terrestrial contamination natural (TCN) and terrestrial contamination artificial (TNA) (Mackinnon et al., 1982; Zolensky et al., 1994). The extra-terrestrial particles include porous chondritic aggregate interplanetary dust particles (IDPs) and non-chondritic IDPs (e.g. Muñoz-Caro et al., 2012). The TNA particles are almost exclusively aluminium-oxide spheres that are solid rocket fuel effluents as part of the US Space Shuttle flights. The origins of TCN particles are varied but appear to be mostly volcanic debris that was lofted naturally (volcanic eruptions; stratospheric winds) or artificially (attached to aircraft and balloons). Identifiable TCN particles were collected in the lower stratosphere (Zolensky et al., 1994) but there are no known processes that could loft TCN particles to the DUSTER collection altitude. It is possible that TCN particles were attached to the balloon skin in earlier flights (Hemenway and Soberman, 1962; Hemenway et al., 1964; Witt et al., 1964; Bigg et al., 1970, 1971). This was highly unlikely in the DUSTER collection of particles with Ca–C–O compositions and the co-occurrence of

structurally modified original carbonate particles and quenched liquid and vapour condensed particles.

We favour an extra-terrestrial origin and cause for the CaO and pure carbon particles described here whereby these Ca–C–O family particles were derived from thermal processing of  $\text{CaCO}_3$  grains in a large, possibly fragile, bolide. In this scenario, the aggregate particles are smoke particles that formed during a bolide event due to dissociation and evaporation of the decelerating meteoroid. Dust aggregation was possible in the dusty, high-temperature environment of a lingering meteoric dust cloud. Meteoric dust particles deposited by bolides can penetrate deep into Earth’s atmosphere. Recent examples include asteroid 2008 TC<sub>3</sub> that detonated at 37-km altitude and left a long-lasting dust cloud that was illuminated by the rising sun (Jenniskens et al., 2009). The dust cloud was observed by satellites (Borovička and Charvát, 2009). This meteoroid was a ureilite that contained graphitic carbon and the long-lasting dust cloud from the carbonaceous chondrite Tagish Lake bolide event (Brown et al., 2000). The Tagish Lake meteorite contains both calcite grains (Zolensky et al., 2002) and organic carbon globules in the carbonate-free part of this meteorite (Nakamura-Messenger et al., 2006).

When meteor events are common, as we know they are (Jenniskens, 2006), it seems to follow that meteoric smoke particles would be abundant. They were identified as the dominant source of aerosol extinction above 35 km and pole ward of 30° latitude (Neely et al., 2011) but so far they have eluded many dedicated high-altitude collection efforts. The predicted meteoric smoke dimensions (Hunten et al., 1980), the sizes of simulated meteoric smoke particles (Plane, 2003; Saunders and Plane, 2011), the remotely

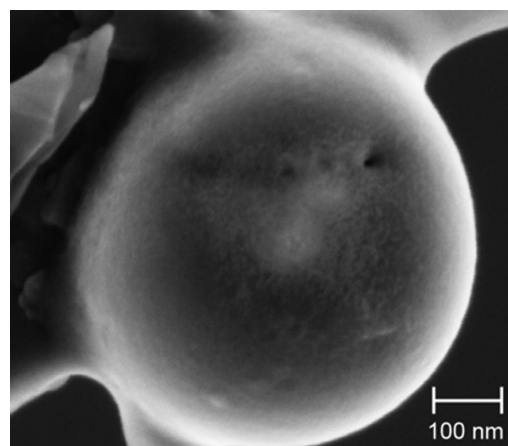


*Fig. 6.* A 610-nm nanosphere extracted from the dolomite decomposition experiment viewed in the FESEM used for this study to determine the collected grain compositions. The pores in this nanosphere are reminiscent of the outgassing pores in the largest sphere of porous aggregate particle (D08\_031).

detected and collected meteoric dust particles (Rietmeijer, 2001), the CaO aggregate (425 nm) and carbon aggregate (290 nm) (this work) and the nanometeorites, that were originally ‘within a larger particle’ >200 nm in size (Hemenway et al., 1961), show that meteoric smoke particles are <1  $\mu\text{m}$ . This means that capturing meteoric smoke particles will require active, balloon-borne collectors with a sub-micron cut-off size in the upper stratosphere. Since May 1982, the NASA Johnson Space Center Cosmic Dust Program routinely samples the lower stratosphere (17–19 km altitudes) using inertial-impact, flat-plate collectors that have a  $\sim 3 \mu\text{m}$  size aerodynamic size cut-off (Zolensky et al., 1994) that prohibits meteoric dust collection.

The meteoroid ablation process causes visible plasma trails that mark their passage through the atmosphere. Spectral analyses of the produced light curves show a wide range of neutral and single ionised atomic species of Na, Mg, Al, Si, K, Ca, Cr, Mn, Fe, Ni as a function of the temperature that is broadly constrained by two thermal regimes, *viz.* the main spectrum with temperatures of 3500–4700 K and the second (or high-temperature) spectrum at about 10 000 K (Borovička, 1993, 2006). Meteor ablation in the lower thermal regime might cause differential ablation whereby the host minerals of the most refractory elements, for example Ca, Al and Ti, are not fully ablated (McNeil et al., 1998; Janches et al., 2009). The most abundant species among the ablated metals maintain mesospheric Na, K, Fe, Mg and  $\text{Mg}^+$  layers, and sporadic Ca layers, at  $\sim 85$ –110 km altitude (McNeil et al., 1998; Murad and Williams, 2002). It was hypothesised that meteoric mesospheric metal condensation produces meteoric smoke particles (Hunten et al., 1980). Indeed, laboratory experiments showed how mesospheric Si and Fe metals in a series of complex, photolysis-driven chemical reactions with  $\text{O}_3$ ,  $\text{O}_2$  and  $\text{N}_2$  will form metal-oxide molecules that when settling through the mesosphere towards the upper stratosphere at  $\sim 40$  km altitude polymerise into nanometre-scale meteoric grains. The condensed nanometre metal-oxide and Mg, Fe-silicate nanoparticles ( $\sim 10$ –200 nm in diameter) in these experiments formed chains of monomict nanoparticles and fluffy aggregates of interconnected three-dimensional networks of such chains (Plane, 2003; Saunders and Plane, 2006, 2011). These experiments demonstrated the feasibility to form the hypothesised meteoric smoke-forming process of  $\text{SiO}_2$  (silica),  $\text{Fe}_2\text{O}_3$  (hematite),  $\text{FeOOH}$  (goethite) and olivine  $[(\text{Mg},\text{Fe})_2\text{SiO}_4]$  nanoparticles. The experimentally obtained grain sizes in these experiments (Saunders and Plane, 2006, 2011) are consistent with those of: (1) goethite particles ( $\sim 400$  nm) collected between 34 and 36 km during May 1985 (Rietmeijer, 1993), and (2) attached to interplanetary dust particles settling through the atmo-

sphere collected at 17–19 km altitude (Rietmeijer, 2001). The 5–30 nm  $\text{Fe}_2\text{O}_3$  and NiO, low-Ni FeNi metal (taenite) nanometeorites, which are compositions that are found in meteorite fusion crusts (Ramdohr, 1967), were collected in the lower stratosphere using impact collectors carried aloft by U2 aircraft in the Arctic on 15 November 1960 (Hemenway et al., 1961). Lacking additional information, their meteoric origin remain uncertain but at least they were collected in the right place and at the right time of the year to increase the probability of collecting meteoric dust (*cf.* Plane, 2003).

It raises the question, ‘Where are the meteoric smoke particles of oxides of Si, Al, Mg, and Ca?’, because these metals along with iron are the most abundant cosmic elements (Anders and Grevesse, 1989). The relative cosmic element abundances alone are no guide to the relative proportions of meteoric smoke particles that can be produced during a meteor event; other factors include metal host phase and the meteoroid petrologic fabric. For example, differential ablation causes a dearth of CaO and  $\text{Al}_2\text{O}_3$  meteoric smoke particles (McNeil et al., 1998; Janches et al., 2009) but their refractory host minerals (Grossman and Larimer, 1974), for example corundum, hibonite and perovskite, should have survived intact or melted. In fast 71.6 km/s Leonid meteoroids, the mineral surface temperature is kept at 1150 K due to rapid surface evaporation, and as a result much of the refractory elements survive in solid, Al-, Ca- and Mg-rich debris (Jenniskens, 2007). Such grains were not yet identified unambiguously during a Leonid meteor storm (Rietmeijer et al., 2003a). The behaviour of meteoric Ca metal in the mesosphere is poorly understood. It probably forms  $\text{Ca}(\text{OH})_2$  molecules but the composition after polymerisation is unknown (Gerding et al., 2000).

The co-occurrence of non-refractory, structurally modified  $\text{CaCO}_3$  grains and smoke aggregates of CaO and pure carbon in this stratospheric dust sample supports a common link to a rapid, high-temperature event that caused survival, (partial) melting and evaporation of calcite and/or aragonite grains followed by the rapid quenching of CaO and pure carbon melt and/or vapour. The most likely ‘closed environment’ for these processes in the Earth’s atmosphere is in dust clouds associated with bolide events wherein grain shattering, melting and evaporation were observed (Borovička and Charvát, 2009). There is observational data that some very bright bolides, for example the Benešov bolide showed faint spectral Ca lines at high altitudes. At low altitudes below 30-km Ca lines were very bright and CaO bands were present in the spectra. Due to its refractory nature, Ca was only partially evaporated at high altitudes but at low altitudes Ca had evaporated completely and both Ca and CaO were observed in the gas phase. Most CaO formed when Ca reacted with

atmospheric oxygen in the cooler wake of this bolide and some fraction of CaO might have ablated directly from the meteoroid (Borovička and Spurný, 1996; Borovička et al., 1998; Berezhnoy and Borovička, 2010).

The CaO and carbon particles discussed here are linked to the behaviour of CaCO<sub>3</sub> grains, which could be calcite, aragonite, or both, during the bolide phase of an incoming meteoroid that should have a petrologic fabric that would allow the ready release of these grains from their host. Preeminent candidates are the friable CI (Carbonaceous Ivuna) and CM (Carbonaceous Murchison) chondrite meteorites, such as the micro-porous, low density (1.67 g/cm<sup>3</sup>), and extremely friable Tagish Lake CI/CM meteorite (Brown et al., 2002). Chemically pure calcite and aragonite with only traces of Mg and Fe are present but rare in the Tonk, Alais, Orgueil and Ivuna CI carbonaceous meteorites but their modal abundances vary widely within and among CIs. Isolated crystals range from <1 µm to 1 mm in size (Frederiksson and Kerridge, 1988; Endress and Bischoff, 1996). In Alais and Ivuna isolated grains have a globular, amoeboid morphology due to spherulitic growth of about 50 µm in diameter. Calcite is often associated with spheroidal magnetite in sub-rounded aggregates approximately 1 mm in size (Frederiksson and Kerridge, 1988). Calcite in CM carbonaceous meteorites contains minor amounts of Fe and/or Mn and is only 2–3% of the total rock and forms isolated micrometre size (Table 1) inclusion-free, subhedral to rounded grains (Benedix et al., 2003; De Leeuw et al., 2010). Aragonite is present in the Murray (CM2) carbonaceous chondrite (Lee and Ellen, 2008). The friable CI/CM Tagish Lake meteorite contains calcite in carbonate replacement structures of CAIs, as well as isolated calcite grains including one 18 µm × 8 µm grain (Zolensky et al., 2002). Carbonates can be found in both anhydrous and hydrated chondritic aggregate IDPs and show a wide range of compositions (Rietmeijer, 1998), including rare Mg-rich calcite grains are 1.4 µm × 1.4 µm and 0.8 µm × 0.5 µm in size (Germani et al., 1990). The smallest calcite grains in CI and CM meteorites approach

the sizes of the largest CaCO<sub>3</sub> grains collected by DUSTER. While calcite is relatively common in CM chondrites, it is a rare mineral constituent in CI chondrites and aragonite is rare in both CI and CM chondrites (Papike, 1998). Thus, the hypothesised bolide that carried the CaCO<sub>3</sub> grains here discussed was probably a CI/CM or a CM meteoroid.

During bolide disintegration these calcite grains become ‘point sources’ for CaO and carbon. To put this into perspective, the mass of the largest grain in porous smoke aggregate (D08\_031) (Fig. 2) would be sufficient to yield about 1 million grains with a 50-nm diameter; or mass of the isolated 18 µm × 8 µm calcite grain in the Tagish Lake meteorite (Zolensky et al., 2002) would be enough to produce 10 million 50-nm diameter grains. There is no shortage of source material to produce this CaO smoke aggregate. Similarly, the available source material would also provide ample amounts of carbon to produce the collected pure carbon aggregate (Fig. 2).

Slow-moving (<20 km/s) bolides of the easily fragmenting carbonaceous chondrite meteorites are prolific producers of dust that can form clouds following the disintegration of a structurally weak, possibly cometary origin, bolide (Ceplecha et al., 1999) such as the dust clouds associated with the Tagish Lake meteorite (Brown et al., 2000) and an unnamed bolide event measured by US DoE sensors on 3 September 2004 (Klekociuk et al., 2005). Meteor disintegration places large amounts of micrometre scale and smaller dust in the stratosphere, and causes dust melting and evaporation, whereby the smallest grains may stay in a suspended mode for considerable time. The deposited dust may survive the ~4000 K temperatures of the ‘main spectrum’ regime (Borovička, 1993) but it will respond to rapidly falling temperatures causing survival with different degrees of dust melting (complete, or only surface melting) and vaporisation. For example, 5 minutes after the luminous bolide phase had ended the temperature of dust settling in the 2008 TC<sub>3</sub> cloud was estimated at >1000 K for at least 1 minute (Borovička and Charvát, 2009). Under these conditions, there can be no presumption of thermodynamic equilibrium, as all chemical reactions in this dynamic environment will be kinetically controlled. Equilibrium melting of calcite and aragonite occurs at 1612 K and 1098 K, respectively. In a flash heating experiment calcite decomposition was achieved at 1223 K just above the calcite decomposition temperature (Han et al., 2007, 2010). This experiment produced smoke particles ranging from about 100 nm to a few hundred nanometres with each aggregate consisting of crystalline CaO nanograins of a few to tens of nanometres in size. While this experiment supports the here-proposed formation of CaO smoke particles, it offers no insight in the formation of pure carbon smoke particles.

Table 1. Range of calcite grain sizes (microns) in selected CM meteorites

CM meteorite	Size range (µm)
Y-791198	20–80
LAP 04796	10–30
Cold Bokkeveld	20–90
Nogoya	20–70
QUE 93005	50–100
QUE 83100	20–80
MET 01070	10–60

Sources: Benedix et al. (2003), De Leeuw et al. (2010) and Papike (1998).



The thermal decomposition of dolomite,  $\text{CaMg}(\text{CO}_3)_2$ , in a low-angle impact experiment produced MgO and CaO nanospheres and carbon melt between approximately 3000 and 4000 K that are more compatible with the thermal conditions conducive to carbonate vaporisation during a bolide event. The experiments fired a 0.375-g Al sphere at 4.9 km/s into a sample of natural dolomite at a  $15^\circ$  angle from the horizontal (Sugita et al., 1998). The impact-generated hypervelocity jets and plumes were monitored for 20  $\mu\text{s}$  by impact flash spectroscopy (IFS) and high-speed imaging. The IFS spectrum showed a very high-continuum background, which is most likely caused by incandescent melt droplets and solid fragments from the projectile and dolomite target (Sugita et al., 1998). The spectral line emissions indicated the presence of CaO and MgO in the gas (Sugita and Schultz, 1999). The reactions in this experiment were: (1)  $\text{CaMg}(\text{CO}_3)_2 = \text{CaO} + \text{MgO} + \text{CO}_2$ , (2)  $\text{CO}_2 = \text{C}_{\text{gas}} + \text{O}_2$ , and (3)  $\text{C}_{\text{gas}} = \text{C}_{\text{solid}}$ . An Analytical Transmission Electron Microscope study of the reaction products of this experiment showed that the reaction products were (1) mostly rounded, condensed CaO and MgO nanograins  $< 50$  nm in diameter; ranging from 4 to  $\sim 200$  nm. When not coated by a carbon rim, these oxide grains form globular grain clusters up to approximately 500 nm in diameter. Co-condensed pure carbons included a considerable variety of hollow globules, massive soot balls, onion shell structures, carbon calabashes, pre-graphitic ribbons and amorphous carbon sheets (Rietmeijer et al., 2003b). There was no evidence for smoke-like structures in this experiment, which might be due to a high grain density in the evolving vapour and dust cloud in the confined volume of the experiment with respect to smoke formation that is considered the real product of the condensation experiment (Rotundi et al., 1998). Another pure carbon particle (D08-029) (Fig. 7) collected by DUSTER shows a sphere resting on a platy substrate, which is a morphology that could easily have arisen from similar kinetically controlled conditions of quenched-liquid or vapour-phase condensation processes, or both, similar to those in this experiment.

This experiment highlighted how high-temperature flash heating will cause carbonate decomposition, melting and evaporation and the co-condensation of metal-oxide (e.g. CaO) nanograins and a plethora of elemental carbon phases at temperatures commensurate with meteoric dust formation and evolution (*cf.* Borovička and Charvát, 2009). Carbon vapour-phase condensation experiments will also produce a variety of elemental carbons that include carbon nanotubes, fullerenic carbon onions and smoke of amorphous carbon nanograins (Rotundi et al., 1998).

The scenario of meteoric smoke formation due to oxidation of mesospheric metals (Hunten et al., 1980; Plane, 2003) does not fit the observations reported here although the sizes for the largest meteoric smoke particles and the smallest CaO and pure carbon nanoparticles overlap. Thus, we will not exclude the possibility that the collected CaO and pure carbon nanograins are evolved by coagulation of meteoric dust particles settling through the mesosphere and in the upper stratosphere. It would require long residence times and high particle number densities (both as yet unknown) for this grain growth process to be efficient. Meteor smoke particles  $< 3$  nm were detected at altitudes from 65 to 85 km (Rapp et al., 2010) and between approximately 35 and 80 km altitudes (Hervig et al., 2009). The meteoric smoke in mesospheric ice particles were composed of carbon (C), wüstite (FeO), or magnesio-wüstite ( $\text{Mg}_x\text{Fe}_{1-x}\text{O}$ ,  $x = 0.1-0.6$ ) (Hervig et al., 2012) but such meteoric smoke particles still remain to be collected and their properties chemical and mineralogical analysed. These particles are perhaps the cause of the meteoritic aerosols collected in the atmosphere between 5 and 19 km altitude (Murphy et al., 1998; Cizco et al., 2001). If so, coagulation and grain growth of meteoric smoke particles is extremely inefficient and the CaO and pure carbon particles collected by DUSTER are not coarsened meteoric smoke particles but were derived from another extra-terrestrial source.

One possible way this could happen is if the bulk components ablated and then formed small meteoric smoke particles at higher altitudes; these would not sediment rapidly, unlike the rather large micron-sized fragments collected at 39 km, which perhaps survived ablation following fragmentation, and sedimented rapidly to the stratosphere.

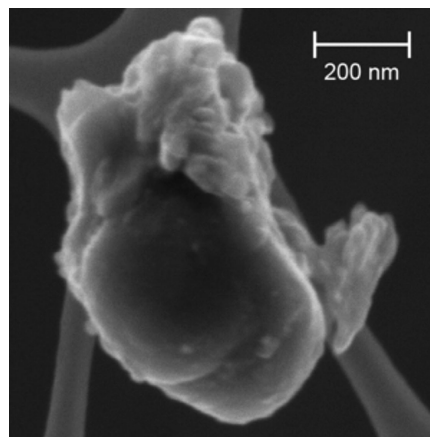


Fig. 7. FESEM image of a composite pure carbon nanoparticle of a sphere resting on a platy substrate (D08-029) collected by DUSTER.

## 5. Conclusions

We collected for the first time the products of the meteor ablation process associated with the disintegration of a fragmenting bolide impacting the Earth's atmosphere. The collected particles that were sampled by flying through the debris cloud of a fireball included intact fragments, thermal eroded fragments, grain melting and vaporisation, vapour-phase condensation forming CaO and pure carbon nanoparticles. Meteoric smoke are the dominant source of aerosol extinction in the upper stratosphere above 35–40 km altitude (Neely et al., 2011) and at lower stratospheric altitudes (Renard et al., 2008, 2010), which supports an ample supply of extra-terrestrial debris to the Earth's atmosphere. Based on the altitude of the collection and the incidental nature of this collection, we conclude that the CaO and carbon nanoparticles originated from a large fragmenting bolide that penetrated deeply into the atmosphere. Classical meteoric smoke was not detected. The solid debris type of particles described here may be referred to as 'meteoritic dust' instead of 'meteoric smoke' that could be restricted to refer to re-condensed extra-terrestrial matter.

## 6. Acknowledgements

The authors thank Dr. Jiri Borovicka and Dr. Peter Jenniskens, and two anonymous reviewers for constructive comments. DUSTER was developed at the Cosmic Physics Laboratory of the University of Naples Parthenope and Istituto Nazionale di AstroFisica where this project was funded by the Italian Space Agency (ASI), PRIN2008/MIUR (Ministero dell'Istruzione dell'Università e della Ricerca), Ministero degli Affari Esteri, and Regione Campania. They thank ASI, ISTAR (International Science Technology and Research) and the Università di Roma 'La Sapienza' for flight and recovery support. F. J. M. R. was supported by grants from the National Aeronautics and Space Administration (LARS NNX11AC36G; Cosmochemistry NNX10AK28G). The authors also thank E. Zona and S. Inarta at the Laboratorio di Fisica Cosmica for technical assistance during DUSTER assembly.

## References

Anders, E. and Grevesse, N. 1989. Abundances of the elements: meteoritic and solar. *Geochim. Cosmochim. Acta.* **53**, 197–214.

Baronnet, A. 1984. Growth kinetics of the silicates. A review of basic concepts. *Fortschritte. Mineralogie.* **62**, 187–232.

Benedix, G. K., Leshin, L. A., Farquhar, J., Jackson, T. and Thiemens, M. H. 2003. Carbonates in CM2 chondrites: constraints on alteration conditions from oxygen isotopic

compositions and petrographic observations. *Geochim. Cosmochim. Acta.* **67**, 1577–1588.

Berezhnoy, A. A. and Borovička, J. 2010. Formation of molecules in bright meteors. *Icarus.* **210**, 150–157.

Bigg, E. K. 2012. Sources of insoluble inclusions in stratospheric sulfate particles. *Meteoritics. Planet. Sci.* **47**, 799–805. DOI: 10.1111/j.1945-5100.2012.01346.x.

Bigg, E. K., Kviz, Z. and Thompson, W. J. 1971. Electron microscope photographs of extra-terrestrial particles. *Tellus A.* **23**, 247–260.

Bigg, E. K., Ono, A. and Thompson, W. J. 1970. Aerosol at altitudes between 20 and 37 km. *Tellus A.* **22**, 550–563.

Borovička, J. 1993. A fireball spectrum analysis. *Astron. Astrophys.* **279**, 627–635.

Borovička, J. 2006. Physical and chemical properties of meteoroids as deduced from observations. In: *Asteroids, Comets, and Meteors* (eds. D. Lazzaro, S. Ferraz-Mello and J. A. Fernández), Cambridge University Press. Proceedings IAU Symposium No. 229, pp. 249–271.

Borovička, J. and Charvát, Z. 2009. Meteoroid observation of the atmospheric entry of 2008 TC3 over Sudan and the associated dust cloud. *Astron. Astrophys.* **507**, 1015–1022.

Borovička, J., Popova, O. P., Nemtchinov, I. V., Spurný, P. and Ceplecha, Z. 1998. Bolides produced by impacts of large meteoroids into the Earth's atmosphere: comparison of theory with observation. I. Benešov bolide dynamics and fragmentation. *Astron. Astrophys.* **334**, 713–728.

Borovička, J. and Spurný, P. 1996. Radiation study of two very bright terrestrial bolides and an application to the comet S-L 9 collision with Jupiter. *Icarus.* **121**, 484–510.

Brown, P. G., Hildebrand, A. R., Zolensky, M. E., Grady, M., Clayton, R. N. and co-authors. 2000. The fall, recovery, orbit, and composition of the Tagish Lake meteorites: a new type of carbonaceous chondrite. *Science.* **290**, 320–325.

Brown, P. G., ReVelle, D. O., Tagliaferri, E. and Hildebrand, A. R. 2002. An entry model for the Tagish Lake fireball using seismic, satellite and infrasound records. *Meteoritics. Planet. Sci.* **37**, 661–675.

Ceplecha, Z., Spalding, E. R., Jacobs, C., ReVelle, O. D., Tagliaferri, E. and co-authors. 1999. In: *Meteoroids 1998* (eds. W. J. Baggaley and V. Porubcan). Proceedings of the International Conference held at Tatranska Lomnica, Slovakia, August 17–21, 1998. Astronomical Institute of the Slovak Academy of Sciences, pp. 37–54.

Ciucci, A. 2011. *Stratospheric Dust Collection by DUSTER (Dust in The Upper Stratosphere Tracking Experiment and Retrieval)*, a balloon-borne instrument and laboratory analyses of collected dust. PhD Thesis. Università degli Studi di Napoli Federico II, Department of Aerospace Engineering, Naples, Italy, 128 p.

Ciucci, A., Palumbo, P., Brunetto, R., Della Corte, V., De Angelis, S. and co-authors. 2011. DUSTER (Dust in the Upper Stratosphere Tracking Experiment and Retrieval): preliminary analysis. *Mem. S. A. It. Suppl. [J. Italian Astron. Soc.]* **16**, 119–124.

Cziczo, D. J., Thomson, D. S. and Murphy, D. M. 2001. Ablation, flux, and atmospheric implications of meteors inferred from stratospheric aerosol. *Science.* **291**, 1772–1775.

- De Angelis, S., Della Corte, V., Baratta, G. A., Rietmeijer, F. J. M., Brunetto, R. and co-authors. 2011. Raman micro-spectroscopy performed on extraterrestrial particles. *Spectroscopy. Lett.* **44**, 549–553.
- De Leeuw, S., Rubin, A. E. and Wasson, J. T. 2010. Carbonates in CM chondrites: complex formational histories and comparison to carbonates in CI chondrites. *Meteoritics. Planet. Sci.* **45**, 513–530.
- Della Corte, V., Palumbo, P., De Angelis, S., Ciucci, A., Brunetto, R. and co-authors. 2011. DUSTER (Dust in the Upper Stratosphere Tracking Experiment and Return): a balloon-borne dust particle collector. *Mem. S.A. It. Suppl.* **16**, 14–21.
- Della Corte, V., Palumbo, P., Rotundi, A., De Angelis, S., Rietmeijer, F. J. M. and co-authors. 2012. In situ collection of refractory dust in the upper stratosphere: the DUSTER Facility. *Space. Sci. Revs.* **169**, 159–180. DOI: 10.1007/s11214-012-9918-9.
- Endress, M. and Bischoff, A. 1996. Carbonates in CI, chondrites: clues to parent body evolution. *Geochim. Cosmochim. Acta.* **60**, 489–507.
- Farlow, N. H., Oberbeck, V. R., Snetsinger, K. G., Ferry, G. V., Polkowski, G. and co-authors. 1981. Size distributions and mineralogy of ash particles in the stratosphere from eruptions of Mount St. Helens. *Science.* **211**, 832–834.
- Frederiksson, K. and Kerridge, J. F. 1988. Carbonates and sulfates in CI chondrites: formation by aqueous activity on the parent body. *Meteoritics.* **23**, 35–44.
- Gerding, M., Alpers, M., Von Zahn, U., Rollason, R. J. and Plane, J. M. C. 2000. Atmospheric Ca and Ca+ layers: midlatitude observations and modeling. *J. Geophys. Res.* **105**(A12), 27131–27146.
- Germani, M. S., Bradley, J. P. and Brownlee, D. E. 1990. Automated thin-film analyses of hydrated interplanetary dust particles in the analytical electron microscope. *Earth. Planet. Sci. Lett.* **101**, 162–179.
- Grossman, L. and Larimer, J. W. 1974. Early chemical history of the solar system. *Revs. Geophys. Space Physics.* **1**, 71–101.
- Han, R., Hiroshi, T. and Shimamoto, T. 2010. Strong velocity weakening and powder lubrication of simulated carbonate faults at seismic slip rates. *J. Geophys. Res.* **115**, B03412.
- Han, R., Shimamoto, T., Hiroshi, T., Ree, J. H. and Ando, J. I. 2007. Ultralow friction of carbonate faults caused by thermal decomposition. *Science.* **316**, 878–881.
- Hawkes, R., Mann, I. and Brown, P. 2005. *Modern Meteor Science: An Interdisciplinary View*. Springer, Dordrecht, The Netherlands.
- Hemenway, C. L., Fullam, A. F., Skrivaneck, R. A., Soberman, R. K. and Witt, G. 1964. Electron microscope studies of noctilucent cloud particles. *Tellus A.* **16**, 96–102.
- Hemenway, C. L., Fullam, E. F. and Phillips, L. 1961. Nanometeorites. *Nature.* **190**, 897–898.
- Hemenway, C. L. and Soberman, R. K. 1962. Studies of micrometeorites obtained from a recoverable sounding rocket. *Astron. J.* **67**, 256–266.
- Hervig, M. E., Deaver, L. E., Bardeen, C. G., Russell, J. M., III, Bailey, S. and co-authors. 2012. The content and composition of meteoric smoke in mesospheric ice particles from SOFIE observations. *J. Atmos. Sol. Terr. Phys.* **84–85**, 1–6.
- Hervig, M. E., Gordley, L. L., Deaver, L. E., Siskind, D. E., Stevens, M. H. and co-authors. 2009. First satellite observations of meteoric smoke in the middle atmosphere. *Geophys. Res. Lett.* **36**, L18805. DOI: 10.1029/2009GL039737.
- Hunten, D. M., Turco, R. P. and Toon, O. B. 1980. Smoke and dust particles of meteoric origin in the mesosphere and stratosphere. *J. Atmos. Sci.* **37**, 1342–1357. DOI: 10.1175/1520-0469(1980)037 <1342:SADPOM >2.0.CO;2.
- Janches, D., Dyruud, L. P., Broadley, S. L. and Plane, J. M. C. 2009. First observation of micrometeoroid differential ablation in the atmosphere. *Geophys. Res. Lett.* **36**, L06101, 1–5.
- Jenniskens, P. 2006. *Meteor Showers and their Parent Comets*. Cambridge University Press, Cambridge, 802 p.
- Jenniskens, P. 2007. Quantitative meteor spectroscopy: elemental abundances. *Adv. Space. Res.* **39**, 491–512.
- Jenniskens, P., Shaddad, M. H., Numan, D., Elsir, S., Kudoda, A. M. and co-authors. 2009. The impact and recovery of asteroid 2008 TC3. *Nature.* **458**, 485–488.
- Klekociuk, A. R., Brown, P. G., Pack, D. E., DeRevelle, D. O., Edwards, W. N. and co-authors. 2005. Meteoritic dust from the atmospheric disintegration of a large meteoroid. *Nature.* **436**, 1132–1135.
- Lee, M. R. and Ellen, R. 2008. Aragonite in the Murray (CM2) carbonaceous chondrite: implications for parent body compaction and aqueous alteration. *Meteoritics. Planet. Sci.* **43**, 1219–1231.
- Love, S. G. and Brownlee, D. E. 1993. A direct measurement of the terrestrial mass accretion rate of cosmic dust. *Science.* **262**, 550–553.
- Mackinnon, I. D. R., McKay, D. S., Nace, G. and Isaacs, A. M. 1982. Classification of the Johnson Space Center stratospheric dust collection. Proceedings of the 13th Lunar and Planetary Science Conference. *J. Geophys. Res.* **87**(Suppl.), A413–A421.
- McNeil, W. J., Lai, S. T. and Murad, E. 1998. Differential ablation of cosmic dust and implications for the relative abundances of atmospheric metals. *J. Geophys. Res.* **103**(D9), 10899–10911.
- Muñoz-Caro, G. M., Rietmeijer, F. J. M., Souza-Egipsy, V. and Valles-González, M. P. 2012. A potentially new type of non-chondritic interplanetary dust particle with hematite, organic carbon, amorphous Na, Ca-aluminosilicate, and Fe-oxide spheres. *Meteoritics. Planet. Sci.* **47**, 248–261.
- Murad, E. and Williams, I. P. 2002. *Meteors in the Earth's Atmosphere*. Cambridge University Press, Cambridge, United Kingdom.
- Murphy, D. M., Thomson, D. S. and Mahoney, M. J. 1998. In situ measurements of organics, meteoritic material, mercury, and other elements in aerosols at 5 to 19 kilometers. *Science* **282**, 1664–1669.
- Nakamura-Messenger, K., Messenger, S., Keller, L. P., Clemett, S. J. and Zolensky, M. E. 2006. Organic globules in the Tagish Lake meteorite: remnants of the protosolar disk. *Science.* **314**, 1439–1442.
- Neely, R. R., III, English, J. M., Toon, O. B., Solomon, S., Mills, M. and co-authors. 2011. Implications of extinction due

- to meteoritic smoke in the upper stratosphere. *Geophys. Res. Lett.* **38**, L24808. DOI: 10.1029/2011GL049865, 2011.
- Papike, J. J. 1998. Planetary Materials. Mineralogical Society of America, Chantilly, VA, 1052 p.
- Plane, J. M. C. 2003. Atmospheric chemistry of meteoric metals. *Chem. Rev.* **103**, 4963–4984.
- Pueschel, R. F., Russell, P. B., Allen, D. A., Ferry, G. V., Snetsinger, K. G. and co-authors. 1994. Physical and optical properties of the Pinatubo volcanic aerosol: aircraft observations with impactors and a sun-tracking photometer. *J. Geophys. Res.* **99**[D6], 12915–12922.
- Ramdohr, P. 1967. Die Schmelzkruste der Meteorieten. *Earth. Planet. Sci. Lett.* **2**, 197–209.
- Rapp, M., Strelnikova, I., Strelnikov, B., Hoffmann, P., Friedrich, M. and co-authors. 2010. Rocket-borne in situ measurements of meteor smoke: charging properties and implications for seasonal variation. *J. Geophys. Res.* **115**, D00I16. DOI: 10.1029/2009JD012725.
- Renard, J. B., Berthet, G., Salazar, V., Catoire, V., Tagger, M. and co-authors. 2010. In situ detection of aerosol layers in the middle stratosphere. *Geophys. Res. Lett.* **37**, L20803. DOI: 10.1029/2010GL044307.
- Renard, J. B., Brogniez, C., Berthet, G., Bourgeois, Q., Gaubicher, B. and co-authors. 2008. Vertical distribution of the different types of aerosols in the stratosphere: detection of solid particles and analysis of their spatial variability. *J. Geophys. Res.* **113**, D21303. DOI: 10.1029/2008JD010150.
- Rietmeijer, F. J. M. 1993. Volcanic dust in the stratosphere between 34 and 36 km altitude during May, 1985. *J. Volc. Geothermal Res.* **55**, 69–83.
- Rietmeijer, F. J. M. 1998. Interplanetary dust particles. In: Planetary Materials, Reviews in Mineralogy (ed. J. J. Papike). Mineralogical Society of America, Chantilly, VA, pp. 2-1–2-95.
- Rietmeijer, F. J. M. 2000. Interrelationships among meteoric metals, meteors, interplanetary dust, micrometeorites, and meteorites. *Meteoritics. Planet. Sci.* **35**, 1025–1041.
- Rietmeijer, F. J. M. 2001. Identification of Fe-rich meteoric dust. *Planet. Space Sci.* **49**, 71–77.
- Rietmeijer, F. J. M., Pfeffer, M. A., Chizmadia, L., Macy, B., Fischer, T. P. and co-authors. 2003a. Leonid dust spheres captured during the 2002 storm? *Lunar Planet. Sci.* **34**, #1358.
- Rietmeijer, F. J. M., Schultz, P. H. and Bunch, T. E. 2003b. Carbon calabashes in a shock-produced carbon melt. *Chem. Phys. Lett.* **374**, 464–470.
- Rose, W. I., Jr., Chuan, R. L., Cadle, R. D. and Woods, D. C. 1980. Small particles in volcanic eruption clouds. *Am. J. Sci.* **280**, 671–696.
- Rose, W. I., Chuan, R. L. and Woods, D. C. 1982. Small particles in plumes of Mount St. Helens. *J. Geophys. Res.* **87**(C7), 4956–4962.
- Rotundi, A., Rietmeijer, F. J. M., Colangeli, L., Mennella, V., Palumbo, P. and co-authors. 1998. Identification of carbon forms in soot materials of astrophysical interest. *Astron. Astrophys.* **329**, 1087–1096.
- Saunders, R. W. and Plane, J. M. C. 2006. A laboratory study of meteor smoke analogues: composition, optical properties and growth kinetics. *J. Atmos. Sol. Terr. Phys.* **68**, 2182–2202.
- Saunders, R. W. and Plane, J. M. C. 2011. A photo-chemical method for the production of olivine nanoparticles as cosmic dust analogues. *Icarus*. **212**, 373–382.
- Sugita, S. and Schultz, P. H. 1999. Spectroscopic characterization of hypervelocity jetting: comparison with standard theory. *J. Geophys. Res.* **104**(E12), 30825–30845.
- Sugita, S., Schultz, P. H. and Adams, M. A. 1998. Spectroscopic measurements of vapor clouds due to oblique impacts. *J. Geophys. Res.* **103**(E8), 19427–19441.
- Testa, J. P., Stephens, J. R., Berg, W. W., Cahill, T. A., Onaka, T. and co-authors. 1990. Collection of microparticles at high balloon altitudes in the stratosphere. *Earth. Planet. Sci. Lett.* **98**, 287–302.
- Witt, G., Hemenway, C. L., Lange, N., Modin, S. and Soberman, R. K. 1964. Composition analysis of particles from noctilucent clouds. *Tellus A.* **16**, 103–109.
- Zolensky, M. E., Nakamura, K., Gounelle, M., Mikouchi, T., Kasama, T. and co-authors. 2002. Mineralogy of Tagish Lake: an ungrouped type 2 carbonaceous chondrite. *Meteoritics. Planet. Sci.* **37**, 737–761.
- Zolensky, M. E., Wilson, T. L., Rietmeijer, F. J. M. and Flynn, G. J. 1994. *Analysis of Interplanetary Dust, AIP Conference Proceedings*. American Institute of Physics, New York, pp. 357.